

# Lawrence Berkeley National Laboratory

## Recent Work

### Title

TRANSITION PROBABILITIES AND MULTIPLE IONIZATIONS OF IONS BY HIGH ENERGY ELECTRON IMPACT

### Permalink

<https://escholarship.org/uc/item/1r60g1xg>

### Author

Hahn, Yukap

### Publication Date

1972-07-01

TRANSITION PROBABILITIES AND MULTIPLE  
IONIZATIONS OF IONS BY HIGH  
ENERGY ELECTRON IMPACT

TWO-WEEK LOAN COPY

*This is a Library Circulating Copy  
which may be borrowed for two weeks.  
For a personal retention copy, call  
Tech. Info. Division, Ext. 5545*

Yukap Hahn and Kenneth M. Watson

July 5, 1972

AEC Contract No. W-7405-eng-48



34

## **DISCLAIMER**

This document was prepared as an account of work sponsored by the United States Government. While this document is believed to contain correct information, neither the United States Government nor any agency thereof, nor the Regents of the University of California, nor any of their employees, makes any warranty, express or implied, or assumes any legal responsibility for the accuracy, completeness, or usefulness of any information, apparatus, product, or process disclosed, or represents that its use would not infringe privately owned rights. Reference herein to any specific commercial product, process, or service by its trade name, trademark, manufacturer, or otherwise, does not necessarily constitute or imply its endorsement, recommendation, or favoring by the United States Government or any agency thereof, or the Regents of the University of California. The views and opinions of authors expressed herein do not necessarily state or reflect those of the United States Government or any agency thereof or the Regents of the University of California.

TRANSITION PROBABILITIES AND MULTIPLE IONIZATIONS OF IONS  
BY HIGH ENERGY ELECTRON IMPACT\*

Yukap Hahn<sup>†</sup> and Kenneth M. Watson

Physics Department and Lawrence Berkeley Laboratory  
University of California, Berkeley, California 94720

July 5, 1972

ABSTRACT

The single-particle model for atoms and ions is used to calculate the transition probabilities to bound and continuum electronic states. The projection operators in the semi-classical approximation derived previously are applied to treat the large numbers of final states involved. Ionization cross sections of atoms and ions by high-energy electron impact are then estimated, which result both from direct transition to the continuum and from inelastic scattering followed by the Auger emission.

I. INTRODUCTION

Electron impact provides a possible mechanism for production of highly ionized beams to be used for injection into heavy ion accelerators. With most of the periodic table and as many as twenty to thirty steps of ionization considered of interest, it is evident that several thousand ionization cross sections may be required to estimate ionization rates. It is also evident that great accuracy is not feasible in the calculation of so many cross sections. The purpose of this paper is to obtain a reasonable estimate in parametrized form for the many required cross sections.

We shall assume the bombarding electrons to have energies large compared with the relevant electronic ionization potentials. Two mechanisms for ionization will be considered; (a) direct transitions to continuum states; (b) excitations of inner shell electrons to excited states followed by Auger emission. Several studies of the fluorescence yield<sup>1-3</sup> indicate that process (b) is no less important than (a) for producing ionization.

To obtain a quantitative estimate of the contribution from the processes (a) and (b), it is desirable first to evaluate the transition probabilities of both inner- and outer-shell electrons to various allowed excited states, including the continuum. For the target atoms and ions, we choose a simple single-particle model. Based on the extensive studies carried out earlier using the Hartree-Fock<sup>4</sup> and Fermi-Thomas models,<sup>5</sup> Green et al.<sup>6</sup> have derived an even simpler model for complex atoms, with analytic potentials of the Coulombic plus Wood-Saxon type. Although rather crude in the prediction of term values, this model is probably sufficient for our present purpose. The form

of potential we have adopted contains essentially one adjustable parameter  $d$  for each core charge  $Z_C$ .

The transition probabilities to a group of excited states and the continuum may be conveniently evaluated using the projection operators derived earlier<sup>7</sup> in the semi-classical approximation. Since the model potential we have chosen is local and in a single-particle form, very little modification is necessary; we have used the simple form  $A_{BO}^k$  in the notation of Ref. 7.

In Sec. II. we define the model potential for the target ions. Since we present the result of our calculations at only several typical values of  $Z_C$  and the degree of ionization  $Z_I$ , the intermediate steps involved in the energy eigenvalue calculations and scaling should be helpful in obtaining results at other values of  $Z_C$  and  $Z_I$ . We give a brief discussion of this in Appendix A. The transition probabilities with dipole coupling are defined in terms of the semi-classical projection operators, and the complete set of transitions allowed by the selection rules and exclusion principle is studied.

The result of Sec. II is then used in Sec. III to estimate the ionization cross sections of ions and atoms by high-energy electron impact. Contributions from the different competing processes mentioned above are evaluated. With the various simplifying approximations which are expected to be valid for high-energy collisions, the transition probabilities evaluated in Sec. II can be directly related to the ionization cross sections.

## II. THE SINGLE-PARTICLE MODEL AND TRANSITION PROBABILITIES

For simplicity, we adopt the single-particle potential for atoms and ions obtained by Green et al.,<sup>6</sup> which was derived by fitting the HF and HFS solutions. Its form is

$$V(r) = \frac{1}{r} [(Z_C - Z_I - 1) Y(r) - Z_C], \quad (2.1)$$

where

$Z_C$  = bare core nuclear charge of an atom or ion,

$Z_I$  = the degree of ionization of the target before the collision, ( $Z_I = 0$  for a neutral atom),

and

$$Y(r) = 1 - \Omega(r), \quad (2.2)$$

where

$$\Omega(r) = [H(e^{r/d} - 1) + 1]^{-1}$$

$$H = \alpha(Z_C - Z_I - 1)^{\nu} d$$

$$\nu = 0.4$$

$$\alpha = 1.00$$

$$m = \hbar = e^2 = 1$$

} for all  $Z_C$  and  $Z_I$ .

Thus, the only parameter which is varied as a function of  $Z_C$  is  $d$ , which is assigned the values<sup>6</sup> given in Table I. (We take Green's values.)

The result of the calculation of the single-particle energies  $E_{n\ell}$  is summarized in Tables II-IV for the value  $Z_C = 10, 20, \dots, 80$ . For each  $Z_C$ , all values of  $Z_I$  which correspond to the filled subshells are considered.

As  $V(r)$  of (2.1) is Coulombic for large values of  $r$ , we expect to have an infinite number of bound states near each ionization threshold. Therefore, the excitation probabilities to these discrete and also to continuum states may be evaluated most conveniently using projection operators. We have shown<sup>7</sup> previously that the projection onto all the bound states generated by the potential  $V(r)$  may be given in a semi-classical approximation by

$$\Lambda_B^{\ell\pm}(r, r') = \frac{1}{\pi r r'} \sin(Pu), \quad (2.3)$$

where

$$P(v) = \left[ -2V(r) - \frac{L_{\pm}^2}{v^2} \right]^{\frac{1}{2}} \quad (2.4)$$

and

$$\begin{aligned} u &= r - r' \\ v &= (r + r')/2 \\ L_{\pm}^2 &= (\ell_{\pm} + \frac{1}{2})^2. \end{aligned} \quad (2.5)$$

In (2.5),  $\ell_{\pm} = \ell \pm 1$  are the angular momenta of the excited states reached by the dipole coupling from the initial state with the angular momentum  $\ell$ .

For a more general case in which the projection onto states which lie between  $E_a$  and  $E_b$  is desired, we have

$$\Lambda_{ab}^{\ell\pm}(r, r') = \frac{1}{\pi r r'} [\sin(P_b u) - \sin(P_a u)] \quad (2.6)$$

where

$$P_a(v) = [2E_a - 2V(v) - L_{\pm}^2 v^{-2}]^{\frac{1}{2}}$$

$$P_b(v) = [2E_b - 2V(v) - L_{\pm}^2 v^{-2}]^{\frac{1}{2}}$$

$$E_a < E_b < 0.$$

Note that, in the rescaled units of Appendix A,

$$P_a(\bar{v}) = \left[ \frac{E_a}{4E_{n\ell}} - \frac{V(\bar{v})}{(E_{n\ell})^{\frac{1}{2}}} - \frac{L_{\pm}^2}{\bar{v}^2} \right]^{\frac{1}{2}} \quad (2.7)$$

with

$$\bar{v} = (s + s')/2, \quad s \equiv 2(E_{n\ell})^{\frac{1}{2}} r, \quad (E_{n\ell} > 0).$$

In particular, we choose in the following  $E_a = E_D$ ,  $E_b = 0$ , which gives  $\Lambda_{ab}^{\ell\pm} \rightarrow \Lambda_D^{\ell\pm}$  for the projections onto states which lie between  $E_D$  and the ionization threshold.

For dipole coupling, the integrals of interest here are then given by

$$M_A^{n\ell\pm} = \langle n\ell | s^2 | n\ell \rangle \quad (2.8)$$

$$M_B^{n\ell\pm} = \langle n\ell | \vec{s} \cdot \Lambda_B^{\ell\pm} \vec{s} | n\ell \rangle \quad (2.9)$$

$$M_C^{nl\pm} = M_A^{nl\pm} - M_B^{nl\pm} \quad (2.10)$$

and

$$M_D^{nl\pm} = \langle nl | \vec{s} \cdot \Lambda_D^{l\pm} \vec{s} | nl \rangle. \quad (2.11)$$

The values for  $E_D$  are chosen such that the transitions are only to the unoccupied levels of given  $l\pm = l \pm 1$ , in accordance with the exclusion principle. Therefore,  $M_D$  corresponds to the correct transition probability to all the unoccupied bound states of the ion with  $Z_C$  and  $Z_I$ , while  $M_B$  includes transitions to all bound levels, some of which are forbidden by the exclusion principle. Throughout the calculation, we have taken  $E_D$  to be the  $E_{nl\pm}$  corresponding to the last filled subshell energies. Table V contains a sample for  $Z_C = 20$ .

The accuracy of the projection operators  $\Lambda_B$  and  $\Lambda_D$  is partly reflected in the integral

$$S_{nl} = \langle nl | \Lambda_B^{l\pm} | nl \rangle, \quad (2.12)$$

which should be unity if  $\Lambda_B^{l\pm}$  were exact and the state  $|nl\rangle$  is contained in  $\Lambda_B^{l\pm}$ . This value is also given in Table V. We refer the readers to Ref. 7 where the accuracy of  $\Lambda_B^{l\pm}$  was studied in detail for several cases where exact results are available for comparison. Except when  $M_B$  or  $M_C$  are very small compared with  $M_A$ , we expect our result to be fairly reliable.

Relativistic corrections are expected to be significant for K-shell electrons when  $Z_C \gtrsim 50$ . Because these inner electrons contribute little to the ionization processes when  $Z_C > 40$ , [see Fig. (2)], we have ignored relativistic corrections to the atomic

structure. The projectile electrons will be treated relativistically, however, in our final results.

Finally, it is of interest to compare the transition probabilities to the continuum calculated here with those for hydrogenic atom given in Ref. 8. For this purpose, we write

$$\tilde{c}_{nl} = \left[ \frac{(\ell + 1) M_C^{nl+} + \ell M_C^{nl-}}{2\ell + 1} \right] (E_{nl}/3), \quad (2.13)$$

where the factor  $1/3$  is the average of the orientation of the dipole operators in (2.8) - (2.10). Table VI contains the result for  $Z_C = 10$  and  $Z_C = 60$ , with  $Z_I = 0$ . Figure 1 also contains the result for  $Z_C = 30$ .

### III. TOTAL IONIZATION CROSS SECTIONS

We consider the collision of a fast electron of momentum  $k_0$  (energy  $\epsilon_0 = k_0^2/2m$  large compared with single orbital ionization energies) with an ion characterized by the charge parameters ( $Z_0, Z_I$ ). The collision leads to a single orbital transition  $\alpha \rightarrow \beta$ , where  $\alpha = n, l$ , etc. The final momentum of the impacting electron is  $k_\beta$ , where

$$\begin{aligned} \epsilon_\beta &= k_\beta^2/2m = \epsilon_0 - \Delta_{\alpha\beta}, \\ \Delta_{\alpha\beta} &= E_\beta - E_\alpha. \end{aligned} \quad (3.1)$$

Neglecting exchange terms involving the impacting electron, we may write the differential cross section in the form given by Mott and Massey<sup>8</sup>

$$I_{\alpha\beta}(\theta) = \left(\frac{m}{2\pi}\right)^2 \frac{k_\beta}{k_0} Z_\alpha \left| \iint d^3r d^3r_0 \phi_\beta^*(r) V_s \phi_\alpha(r) e^{i\vec{q}\cdot\vec{r}_0} \right|^2, \quad (3.2)$$

where the  $\phi$ 's are single electron orbital states,

$$\vec{q} = \vec{k}_0 - \vec{k}_\beta = q \hat{n}, \quad (3.3)$$

$\theta$  is the scattering angle, and

$$V_s = e^2 / |\vec{r}_0 - \vec{r}|. \quad (3.4)$$

We take  $Z_\alpha$  to be the number of electrons in the shell  $\alpha = (n, l)$ .

For high energy impacts, we may use the dipole approximation<sup>8</sup>

$$\begin{aligned} \int d^3r_0 e^{i\vec{q}\cdot\vec{r}_0} V_s &= \frac{4\pi e^2}{q^2} e^{i\vec{q}\cdot\vec{r}} \\ &\approx \frac{4\pi e^2}{q^2} (1 + i\vec{q}\cdot\vec{r}\hat{n}) \end{aligned} \quad (3.5)$$

Thus,

$$I_{\alpha\beta}(\theta) = 8\pi \left(\frac{k_\beta}{k_0 q^2}\right) Z_\alpha M_{\alpha\beta}, \quad (3.6)$$

where

$$M_{\alpha\beta} = \left| \int d^3r \phi_\beta^*(r) \phi_\alpha(r) \vec{r}\cdot\hat{n} \right|^2 / (a_0)^2. \quad (3.7)$$

Now,

$$k_0 k_\beta \sin\theta d\theta = q dq \approx k_0^2 \sin\theta d\theta, \quad (3.8)$$

so we may introduce

$$J_{\alpha\beta}(q) dq = 2\pi I_{\alpha\beta}(\theta) k_\alpha k_\beta \sin\theta d\theta / q, \quad (3.9)$$

or the total cross section

$$\sigma_{\alpha\beta}(k_\alpha) = \int_{q_{\min}}^{q_{\max}} J_{\alpha\beta}(q) dq \approx \frac{4\pi Z_\alpha}{k_0^2} M_{\alpha\beta} \ln\left(\frac{4\epsilon_0}{\Delta_{\alpha\beta}}\right). \quad (3.10)$$

Here, we have used high energy, nonrelativistic kinematics<sup>9</sup> to determine the limits on  $q$  as

$$\begin{aligned} q_{\min} &\approx m \Delta_{\alpha\beta} / k_\alpha \\ q_{\max} &\approx (2mE_0)^{\frac{1}{2}} \end{aligned} \quad (3.11)$$



We consider first the direct ionization to continuum states. When the expression (3.9) for  $\sigma_{\alpha\beta}^C$  is summed over all available final states, we have

$$\begin{aligned} \sigma_{\alpha}^C(k_{\alpha}) &= \sum_{\beta} \sigma_{\alpha\beta}^C \approx \sum_{\beta} \frac{4\pi Z_{\alpha}}{k_{\alpha}^2} M_{\alpha\beta}^C \ln\left(\frac{4\epsilon_{\alpha}}{\Delta_{\alpha\beta}^C}\right) \\ &\equiv \frac{4\pi Z_{\alpha}}{k_{\alpha}^2} \ln\left(\frac{4\epsilon_{\alpha}}{\Delta_{\alpha}^C}\right) M_C^{\alpha}, \end{aligned} \quad (3.12)$$

where

$$M_C^{\alpha} = \sum_{\beta} M_{\alpha\beta}^C, \quad \alpha = (n, \ell) \quad (3.13)$$

$\Delta_{\alpha}^C$  = the average excitation energy defined by (3.12).

Since both  $M_C^{n\ell+}$  and  $M_C^{n\ell-}$  are involved in our case, we replace  $M_C^{\alpha}$  in (3.12) by its average

$$\bar{M}_C^{n\ell} \equiv \frac{1}{3(2\ell+1)} [(\ell+1) M_C^{n\ell+} + \ell M_C^{n\ell-}] \equiv \bar{M}_C^{\alpha} \quad (3.14)$$

and set

$$Z_{\alpha} \equiv Z_{n\ell} = 2(2\ell+1), \quad \text{for each closed subshell.} \quad (3.15)$$

Thus, combining (3.12) - (3.15), we finally have

$$\sigma_{\alpha}^C(k_{\alpha}) = (\pi a_0^2) \frac{4Z_{\alpha}}{(k_{\alpha} a_0)^2} \ln\left(\frac{4\epsilon_{\alpha}}{\Delta_{\alpha}^C}\right) \bar{M}_C^{\alpha}, \quad (\text{NR}) \quad (3.16)$$

and thus

$$\sigma_{\alpha}^C(Z_C, Z_I, E) = \sum_{\alpha} \sigma_{\alpha}^C. \quad (3.17)$$

As discussed earlier, the ionization of the target ions is also possible through the excitation of an inner-shell electron followed by an Auger transition. This is then related to the transition matrix elements  $M_D^{n\ell\pm}$  to all the allowed bound state levels and also to the fluorescence yield. If we denote by  $W_{\alpha}$  the probability that an Auger transition will follow excitation from the orbital state  $\alpha$ , the cross section for ionization following collisional excitation is

$$\sigma_{\alpha}^A(k_{\alpha}) = (\pi a_0^2) \frac{4Z_{\alpha}}{(k_{\alpha} a_0)^2} \ln\left(\frac{4\epsilon_{\alpha}}{\Delta_{\alpha}^B}\right) \bar{M}_D^{\alpha} W_{\alpha} \quad (\text{NR}) \quad (3.18)$$

which follows from the argument similar to that was used to obtain (3.16), and thus

$$\sigma_{\alpha}^A(Z_C, Z_I, E) = \sum_{\alpha} \sigma_{\alpha}^A. \quad (3.19)$$

In (3.18),  $\bar{M}_D^{\alpha}$  are given by the fluorescence yield  $Y_{\alpha}$  as  $W_{\alpha} = 1 - Y_{\alpha}$ , and the actual values used in our calculation are given in Fig. 2, with  $W_{\alpha} = 1$  for  $n \geq 3$ ;  $\Delta_{\alpha}^B$  is the average excitation energy of the  $\alpha$ th subshell, and

$$\bar{M}_D^{\alpha} = \frac{1}{3(2\ell+1)} [(\ell+1) M_D^{n\ell+} + \ell M_D^{n\ell-}]. \quad (3.20)$$

The total ionization cross section is finally given by

$$\sigma^I(Z_C, Z_I, E) = \sum_{\alpha} (\sigma_{\alpha}^C + \sigma_{\alpha}^A) \quad (3.21)$$

for each set of parameters  $Z_C$ ,  $Z_I$ , and  $E$ .

In actual calculation, we simply used

$$\Delta_{\alpha}^C \approx \Delta_{\alpha}^B \approx E_I \quad (3.22)$$

where  $E_I$  is the ionization potential for the electron in the highest filled subshell. Since the cross sections depend on  $\Delta$  only logarithmically, the choice (3.22) is not expected to affect the result drastically. An improved treatment of the log factor is possible, however, and this is outlined in Appendix B, where a procedure to estimate the average excitation energy is presented.

When the incident electron is relativistic, we have to modify (3.16) and (3.18) slightly as<sup>8</sup>

$$\log\left(\frac{4\epsilon_{\alpha}}{\Delta_{\alpha}}\right) \rightarrow \left[ \log\left(\frac{4\epsilon_{\alpha}\gamma}{\Delta_{\alpha}}\right) - \beta^2 \right] \quad (3.23)$$

and

$$k_{\alpha} a_0 \rightarrow \beta/\alpha_0, \quad (3.24)$$

where

$$\alpha_0 = \frac{e^2}{\hbar c} = \frac{1}{137}$$

$$\gamma = (1 - \beta^2)^{-\frac{1}{2}}, \quad \beta = v/c.$$

Thus, we have explicitly, at high energies with relativistic electron beams and with  $E = \gamma mc^2$ ,

$$\sigma_{\alpha}^C = (\pi a_0^2) \frac{4\alpha_0^2}{\beta^2} \left[ \ln\left(\frac{2\beta^2 E}{\Delta_{\alpha}^C}\right) - \beta^2 \right] Z_{\alpha} \bar{M}_C^{\alpha}, \quad (ER) \quad (3.25)$$

$$\sigma_{\alpha}^A = (\pi a_0^2) \frac{4\alpha_0^2}{\beta^2} \left[ \ln\left(\frac{2\beta^2 E}{\Delta_{\alpha}^B}\right) - \beta^2 \right] Z_{\alpha} \bar{M}_D^{\alpha} W_{\alpha}, \quad (ER). \quad (3.26)$$

In Table VII, both nonrelativistic forms (3.16), (3.18), and the extreme relativistic forms (3.25), (3.26) of cross sections are used to calculate the total ionizations. The result at  $\epsilon_0 = 1$  KeV and at 10 KeV seems to agree reasonably well with the earlier calculations and also with the experimental value. We note that the contribution of  $\sigma^A$  is not negligible.

Individual values of  $\sigma^C$  and  $\sigma^A$  for various  $Z_C$  and  $Z \equiv Z_C - Z_I$  are presented in Fig. 3. For given  $Z$ ,  $\sigma^C$  seems to dominate at small  $Z_C$ , but this trend is reversed for large  $Z_C$ , with  $\sigma^A$  dominating at high  $Z_C$ . The total ionization cross section  $\sigma^I$  is given in Fig. 4 for an electron energy of 20 Mev. The cross section at other energies may be scaled from Fig. 4 and Eqns. (3.10), (3.18), (3.25), and (3.26).

#### IV. DISCUSSION

The ionization cross sections that we have obtained in Section III are based on a rather crude model for the electron orbital states. The comparisons in Tables VI and VII with the corresponding exact calculations given in Ref. 8 (for hydrogen, however, so that direct comparison is not possible) and with some experimental cross sections provide an indication of the accuracy of our cross sections. We have made several of the 'standard' high energy approximations and these of course limit the energy range over which our expressions can be used.

The previous estimates<sup>3</sup> of  $\sigma^I$  do not include the contribution of  $\sigma^A$ , which requires both  $\bar{M}_D^\alpha$  and  $W_\alpha$ . Since  $\sigma^A$  seems to dominate the ionization cross sections at high  $Z_C$ , any agreement existed previously between the theoretical calculations and experiments could be fortuitous.

#### ACKNOWLEDGMENT

We would like to thank Drs. M. Rotenberg and F. Gilmore for some of the recent references on the Thomas-Fermi model and Auger transition calculations, and also Dr. Hans Mark for sending us a preprint of a forthcoming review of Auger processes and fluorescent yields. The present calculation has been carried out at the request of Dr. L. J. Laslett and the E. R. A. group. One of us (YH) would like to thank the members of the Physics Department and Lawrence Berkeley Laboratory for their hospitality.

APPENDIX A

The calculation of the eigenvalues and eigenfunctions with the local potential  $V(r)$  given in Sec. II is well known, but we briefly describe the procedure used in our calculation so that results at other values of  $Z_C$  and  $Z_I$  than those presented here could be readily reproduced.

The single-particle energies and wave functions are calculated in the usual way by solving the radial equation

$$\left[ -\frac{d^2}{dr^2} + \frac{\ell(\ell+1)}{r^2} + 2V(r) + E_{n\ell} \right] R_{n\ell}(r) = 0, \quad (A.1)$$

where  $E_{n\ell}$  is given in Rydberg units. Since a large variation in  $Z_C$  and  $E_{n\ell}$  is involved, we rescale the variable  $r$  such that (A.1) becomes

$$\left[ -\frac{d^2}{ds^2} + \frac{2V(s)}{2(E_{n\ell})^{\frac{1}{2}}} + \frac{1}{4} + \frac{(\ell + \frac{1}{2})^2 - \frac{1}{4}}{s^2} \right] R_{n\ell}(s) = 0, \quad (A.2)$$

with

$$s = 2(E_{n\ell})^{\frac{1}{2}} r, \quad (E_{n\ell} > 0)$$

$$V(s) = V\left[ r \rightarrow s, \quad d \rightarrow d' = 2(E_{n\ell})^{\frac{1}{2}} d \right].$$

The solutions obtained by integrating (A.2) in from the large values of  $s$  and out from  $s \approx 0$  are matched at  $s = s_0$ ,  $s_0 \approx 20h$  with  $h = 0.2$  in the above unit.

The starting values for the integrations are calculated as follows:

(a)  $s = 0$  region:

Using the expansion of the regular Whittaker function,<sup>10</sup>

$$R_{n\ell}(s) \approx M_{km}(s) = s^{\frac{1}{2}+m} e^{-\frac{1}{2}s} \left\{ 1 + \frac{\frac{1}{2} + m - k}{1!(2m+1)} s + \frac{\left(\frac{1}{2} + m - k\right)\left(\frac{3}{2} + m - k\right)}{2!(2m+1)(2m+2)} s^2 + \dots \right\}, \quad (A.3)$$

where

$$k = Z_C / (E_{n\ell})^{\frac{1}{2}}$$

$$m = \frac{1}{2}.$$

That is, the dominant part of  $V(r)$  near  $r = 0$  is taken to be purely Coulombic with the charge  $Z_C$ . The correction to the wave function coming from the non-Coulombic part of  $V(s)$  is then included by integrating out with the finer mesh size  $h' = 0.1h$ . In this way, the starting values of  $R_{n\ell}$  and  $R'_{n\ell}$  at  $s = h$  for further integration outward with  $\Delta s = h$  are generated.

(b)  $s$  large:

Since the core charge  $Z_C$  is in general screened by the  $(Z_C - Z_I - 1)$  electrons, we have to modify the value of  $k$  in the region of large  $s$ , as

$$k \rightarrow \kappa = (Z_I + 1) / (E_{n\ell})^{\frac{1}{2}}$$

$$m = \frac{1}{2}.$$

Thus, we have<sup>10</sup>

$$R_{nl} \approx W_{km}(s) = e^{-\frac{s}{2}} s^{\kappa} \left\{ 1 + \frac{m^2 - (\kappa - \frac{1}{2})^2}{1!s} + \frac{\left\{ m^2 - (\kappa - \frac{1}{2})^2 \right\} \left\{ m^2 - (\kappa - \frac{3}{2})^2 \right\}}{2! s^2} + \dots \right\} \quad (A.4)$$

Typically, the starting values are evaluated at  $s \approx 27$  in the rescaled atomic units.

(c) The matching of the logarithmic derivatives is made at  $s = s_0 = 20h$ ,  $h = 0.2$ , except when they are very small in this region. The value of  $E_{nl}^{(t)}$  guessed initially is corrected by the formula

$$E_{nl} \approx E_{nl}^{(t)} + \Delta_{nl}$$

where

$$\Delta_{nl} = \left[ \int_0^{s_0} u_t^2 ds / (u_t^2|_{s=s_0}) + \int_{s_0}^{\infty} v_t^2 ds / (v_t^2|_{s=s_0}) \right] \cdot [v_t'/v_t - u_t'/u_t]_{s=s_0}^{-1} \quad (A.5)$$

In (A.5),  $u_t$  and  $v_t$  are the functions obtained by integrating out and in, respectively. With a reasonable initial guess on  $E_{nl}^{(t)}$ , the procedure converged within five iterations to an accuracy of one part in  $10^4$ . Note that the variable  $r$  is rescaled as  $E_{nl}$  is changed.

In view of the crudeness of the model used, the eigenvalues  $E_{nl}$  are not expected to be very accurate, especially for the higher excited states. In fact, the variations among the values obtained with

different models are substantial. Therefore,  $R_{nl}$  and  $E_{nl}$  are calculated here only to the accuracy which is sufficient to give a rough estimate of the excited states involved.

APPENDIX B

The average excitation energies  $\Delta_\alpha^B$  and  $\Delta_\alpha^C$  introduced in Sec. III may be estimated more accurately if we write, by definition,

$$M_B^{(\alpha)} \ln \left( \frac{4\epsilon_\alpha}{\Delta_\alpha^B} \right) \equiv \sum_\beta' |\langle \alpha | \vec{r}_1 \cdot \vec{n} | \beta \rangle|^2 \ln \left( \frac{4\epsilon_\alpha}{E_\alpha - E_\beta} \right), \quad (B.1)$$

and similarly for  $\Delta_\alpha^C$  where  $M_C^{(\alpha)}$  is given by (3.13). The range of the  $\beta$ -sum is such that

$$\begin{aligned} 0 < E_\alpha - E_D < \Delta_\alpha^B < E_D \\ E_\alpha < \Delta_\alpha^C < \infty. \end{aligned} \quad (B.2)$$

The right-hand side of (B.1) may be evaluated using the identity

$$\begin{aligned} \ln \left( \frac{4\epsilon_\alpha}{E_\alpha - E_\beta} \right) &= \ln \left( \frac{4\epsilon_\alpha}{E_\alpha} \right) + \ln \left( \frac{E_\alpha}{E_\alpha - E_\beta} \right) \\ &= \ln \left( \frac{4\epsilon_\alpha}{E_\alpha} \right) + \int_0^1 dc \left\langle \beta \left| \frac{D}{E_\alpha - cD} \right| \beta \right\rangle \end{aligned} \quad (B.3)$$

where the operator  $D$  is defined such that

$$\begin{aligned} D|\beta\rangle &= E_\beta|\beta\rangle, \quad (E_\beta > 0 \text{ for bound states}), \\ [D, \Lambda_\beta] &= 0 = [D, \Lambda_C]. \end{aligned} \quad (B.4)$$

Therefore, (B.1) may be rewritten as

$$\begin{aligned} \ln \left( \frac{4\epsilon_\alpha}{\Delta_\alpha^B} \right) &= \frac{1}{M_B^{(\alpha)}} \left\{ \langle \alpha | \vec{r}_1 \cdot \vec{n} \Lambda_\beta \vec{r}_1 \cdot \vec{n} | \alpha \rangle \ln \left( \frac{4\epsilon_\alpha}{E_\alpha} \right) \right\} \\ &+ \int_0^1 dc \langle \alpha | \vec{r}_1 \cdot \vec{n} \tilde{G}_\alpha^{B \cdot D} \vec{r}_1 \cdot \vec{n} | \alpha \rangle \end{aligned}, \quad (B.5)$$

where

$$\tilde{G}_\alpha^{B \cdot D} \equiv \left( \frac{1}{E_\alpha - cD} \right)_B. \quad (B.6)$$

As in Sections II and III, we may now replace the  $\Lambda_B$  and  $\tilde{G}_\alpha^{B \cdot D}$  by their semiclassical approximations. That is<sup>7</sup>,

$$\Lambda_B \rightarrow \frac{1}{2\pi^2 u} \sin(P(v)u) \quad (B.7)$$

and

$$\tilde{G}_\alpha^{B \cdot D} \rightarrow \frac{1}{\pi^2 u} \int_0^{P(v)} \frac{p dp \sin(pu)}{2E_\alpha - cp^2 - 2cV(v)}, \quad (B.8)$$

where  $V(v)$  is the single-particle model potential defined in Sec. II. Similar expressions can be derived for  $\Delta_\alpha^C$  by replacing in (B.5) the subspace label  $B$  by  $C$ .

We do not consider (B.5) further in this paper, since  $\Delta_\alpha^B$  and  $\Delta_\alpha^C$  appear in the cross sections only logarithmically so that their effect would not be expected to change the overall estimate of  $\sigma$  in any serious way.

FOOTNOTES AND REFERENCES

- \* Research supported in part by the U. S. Atomic Energy Commission and by the Air Force Office of Scientific Research, Office of Aerospace Research, United States Air Force, under Contract #F44620-70-C-0028.
- + On sabbatical leave from the Physics Department, University of Connecticut, Storrs, Connecticut 06268. Participating guest, Lawrence Berkeley Laboratory.
1. E. J. McGuire, Phys. Rev. A5, 1052 (1972), and A3, 587 (1971), where many of the earlier references could be found; also W. Fink, R. C. Jopson, H. Marks, and C. D. Swift, Rev. Mod. Phys. 38, 513 (1966); W. Bambynek, B. Crasemann, F. W. Funk, H. U. Freund, H. Mark, C. D. Swift, R. E. Price, and P. V. Rao, preprint, Ames Research Center, 1972.
  2. V. O. Kostroun, M. H. Chen, and B. Crasemann, Phys. Rev. A3, 533 (1971), and also *ibid* A4, 1 (1971).
  3. See, for example, K. Omidvar, H. L. Kyle, and E. C. Sullivan, Phys. Rev. A5, 1174 (1972).
  4. F. Herman and S. Skillman, Atomic Structure Calculations (Prentice-Hall, Inc., Englewood Cliffs, New Jersey, 1963).
  5. For example, R. Latter, Phys. Rev. 99, 510 (1955); J. C. Stewart and M. Rotenberg, *ibid* A140, 1508 (1965).
  6. A. E. S. Green, D. L. Sellin, and A. S. Zachor, Phys. Rev. 184, 1 (1969).
  7. Y. Hahn and K. M. Watson, Phys. Rev. A6, (1972).
  8. N. F. Mott and H. S. W. Massey, The Theory of Atomic Collisions (Oxford Press, 1965), Chapter 16.

9. Corrections for a relativistic impacting electron will be introduced later.
10. E. T. Whittaker and G. N. Watson, A Course of Modern Analysis (Cambridge University Press, 1952), pp. 337-342.

Table I. The parameter  $d$  in the single-particle potential as given in Ref. 6. The same values are used for all  $Z_I$  at each  $Z_C$ . (Atomic units.)

$Z_C$	$d$
10	0.500
20	1.154
30	0.612
40	0.866
50	0.841
60	0.938
70	0.654
80	0.671

Table II. The energy eigenvalues calculated with the single-particle model potential of Ref. 6, for the core charges  $Z_C = 10, 20, 30,$  and  $40$ . The values of  $Z_I$  are chosen for all closed subshells. The energies  $E_{nl}$  are given in Rydbergs.

$Z_C$	$Z_I$	1s	2s	2p	3s	3p	3d	4s	4p
10	8	98.02							
	6	91.45	18.50						
	0	64.20	3.38	1.88					
20	18	398.0							
	16	391.4	92.84						
	10	362.0	72.25	70.70					
	8	350.4	64.64	62.51	20.88				
	2	311.4	40.79	36.80	7.70	6.58			
30	28	898.0							
	26	891.0	216.6						
	20	859.8	191.7	190.7					
	18	847.2	182.3	180.7	68.10				
	12	804.9	151.8	148.4	48.15	46.59			
	2	723.1	96.9	89.7	15.65	13.38	7.60		
40	38	1598							
	36	1591	391.3						
	30	1559	365.2	364.6					
	28	1547	355.1	354.0	142.8				
	22	1503	322.1	319.2	119.5	117.2			
	12	1419	261.1	254.5	79.0	76.0	70.0		
	10	1401	248.2	240.8	70.8	67.6	60.0	25.7	
	4	1343	208.7	198.6	46.5	42.7	33.4	11.6	10.7



Table III. Same as Table II, for  $Z_C = 50$  and 60.

$Z_C$	$Z_I$	1s	2s	2p	3s	3p	3d	4s	4p	4d	4f
50	48	2498									
	46	2491	616								
	40	2459	588	588							
	38	2446	578	577	239						
	32	2402	542	540	213	212					
	22	2315	476	480	166	164	156				
	20	2296	462	456	157	150	146	68			
	14	2237	419	410	128	124	113	49	48		
	4	2130	343	329	79	73	60	19	18	13	
60	58	3598									
	56	3591	890								
	50	3559	862	862							
	48	3545	851	851	359						
	42	3501	814	813	331	330					
	32	3413	745	740	280	277	270				
	30	3393	730	724	269	266	258	126			
	24	3333	683	676	237	233	222	104	102		
	14	3224	602	590	181	175	161	67	65	58	
	6	3131	534	518	136	129	111	39	37	29	19
	0	3057	481	462	102	95	74	19	18	10	

Table IV. Same as Table II, for  $Z_C = 70$  and 80.

$Z_C$	$Z_I$	1s	2s	2p	3s	3p	3d	4s	4p	4d	4f	5s	5p	5d	
70	68	4898													
	66	4891	1215												
	60	4858	1185	1186											
	58	4845	1174	1174	500										
	52	4799	1135	1134	470	469									
	42	4710	1061	1058	413	411	404								
	40	4690	1046	1041	401	399	391	195							
	34	4629	997	990	365	362	352	169	168						
	24	4518	910	899	303	298	283	126	124	116					
	10	4347	780	763	214	206	184	67	64	54	40				
	2	4242	703	681	162	153	127	35	33	22	8.7	5.8			
	80	78	6398												
		76	6391	1589											
70		6358	1561												

Table continued next page

Table IV continued.

$Z_C$	$Z_I$	1s	2s	2p	3s	3p	3d	4s	4p	4d	4f	5s	5p	5d
80	68	6344	1547	1549	665									
	62	6299	1508	1508	633	633								
	52	6209	1432	1429	574	572	566							
	50	6189	1416	1412	561	559	552	281						
	44	6127	1365	1360	523	520	510	253	252					
	34	6014	1275	1266	456	451	436	205	203	194				
	20	5841	1140	1124	359	351	329	138	135	123	107			
	12	5735	1059	1039	302	293	267	100	97	84	66	37		
	2	5597	954	929	231	220	189	54	51	38	19	10.1	10.0	

Table V. The transition probabilities and overlap integrals for  $Z_C = 20$ , and in the dipole approximation. All values are given in atomic units.  $Z_I$  denotes the degree of ionization.

$Z_I$	$n_l$	$l \pm$	S	$M_A$	$M_B$	$M_C$	$M_D$
18	10	1	0.922	0.008	0.006	0.002	0.006
16	10	1	0.920	0.008	0.006	0.002	0.006
	20	1	0.960	0.107	0.104	0.003	0.104
10	10	1	0.914	0.008	0.005	0.002	0.001
	20	1	0.952	0.116	0.112	0.005	0.095
	21	0	0.960	0.085	0.085	0.000	0.044
	21	2	0.960	0.085	0.070	0.015	0.070
8	10	1	0.912	0.008	0.005	0.002	0.001
	20	1	0.949	0.121	0.115	0.006	0.098
	21	0	0.958	0.089	0.089	0.000	0.002
	21	2	0.958	0.089	0.071	0.018	0.071
	30	1	0.962	0.731	0.720	0.010	0.719
2	10	1	0.902	0.008	0.005	0.003	0.000
	20	1	0.929	0.142	0.130	0.012	0.008
	21	0	0.943	0.110	0.110	0.000	0.002
	21	2	0.943	0.110	0.068	0.042	0.068
	30	1	0.936	1.164	1.114	0.050	0.765
	31	0	0.955	1.149	1.151	0.002	0.724
	31	2	0.955	1.149	1.024	0.126	1.024

Table VI. Comparison of the transition probabilities to the continuum as calculated here and those given in Ref. 8.  $\tilde{c}_{nl}$  is defined by (2.13).

$Z_C$	$Z_I$	$nl$	$c_{nl}$	$\tilde{c}_{nl}$
10	0	10	0.28	0.36
		20	0.21	0.30
		21	0.13	0.20
60	0	10	0.28	0.30
		20	0.21	0.14
		21	0.13	0.32
		30	0.17	0.14
		31	0.14	0.20
		32	0.07	0.27
		40	0.15	0.18
		41	0.13	0.22
		42	0.09	0.54

Table VII. The ionization cross sections  $\sigma^C$ ,  $\sigma^A$ , and  $\sigma^I$  in units of  $\pi a_0^2$ , where  $a_0 = \text{Bohr radius}$ .  $\sigma^B$  corresponds to total excitation cross section to all the bound states, where the effect of the exclusion principle is neglected. The experimental values are summarized in Ref. 3.

$$\underline{Z_C = 10, Z_I = 0, Z = Z_C - Z_I = 10}$$

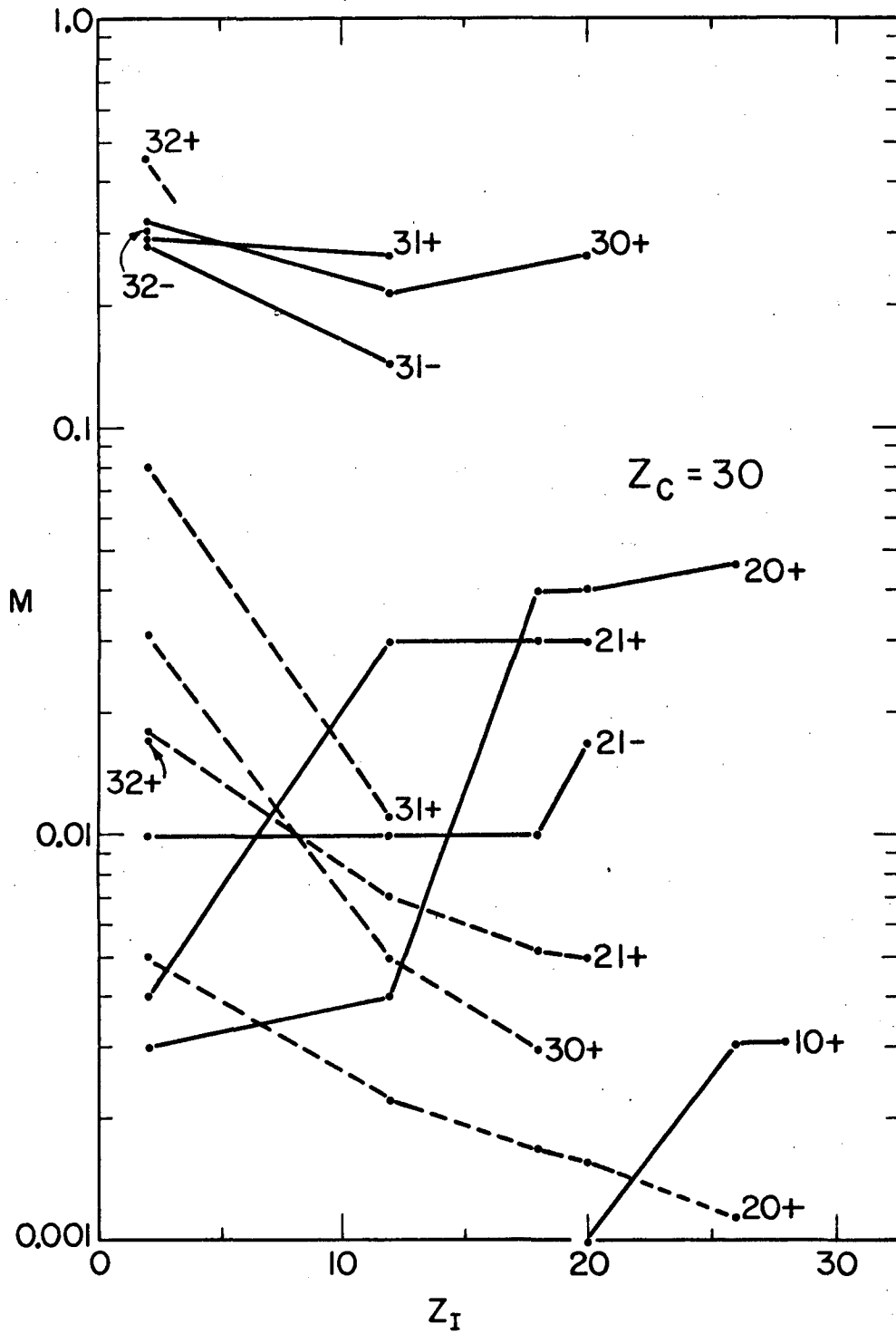
$$\begin{aligned} \epsilon_0 = 1 \text{ KeV:} & \quad \sigma^B = 0.363 \\ & \quad \sigma^C = 0.396 \\ & \quad \sigma^A = 0.087 \\ & \quad \sigma^I = 0.483 \end{aligned} \quad \text{Exp. } \sigma^I \approx 0.35 \sim 0.43$$

$$\begin{aligned} \underline{\epsilon_0 = 10 \text{ KeV:}} & \quad \sigma^B = 0.053 \\ & \quad \sigma^C = 0.058 \\ & \quad \sigma^A = 0.013 \\ & \quad \sigma^I = 0.071 \end{aligned} \quad \text{Exp. } \sigma^I \approx 0.07$$

$$\begin{aligned} \underline{E = 20 \text{ MeV:}} & \quad \sigma^B = 0.0049 \\ & \quad \sigma^C = 0.0083 \\ & \quad \sigma^A = 0.0019 \\ & \quad \sigma^I = 0.0102 \end{aligned}$$

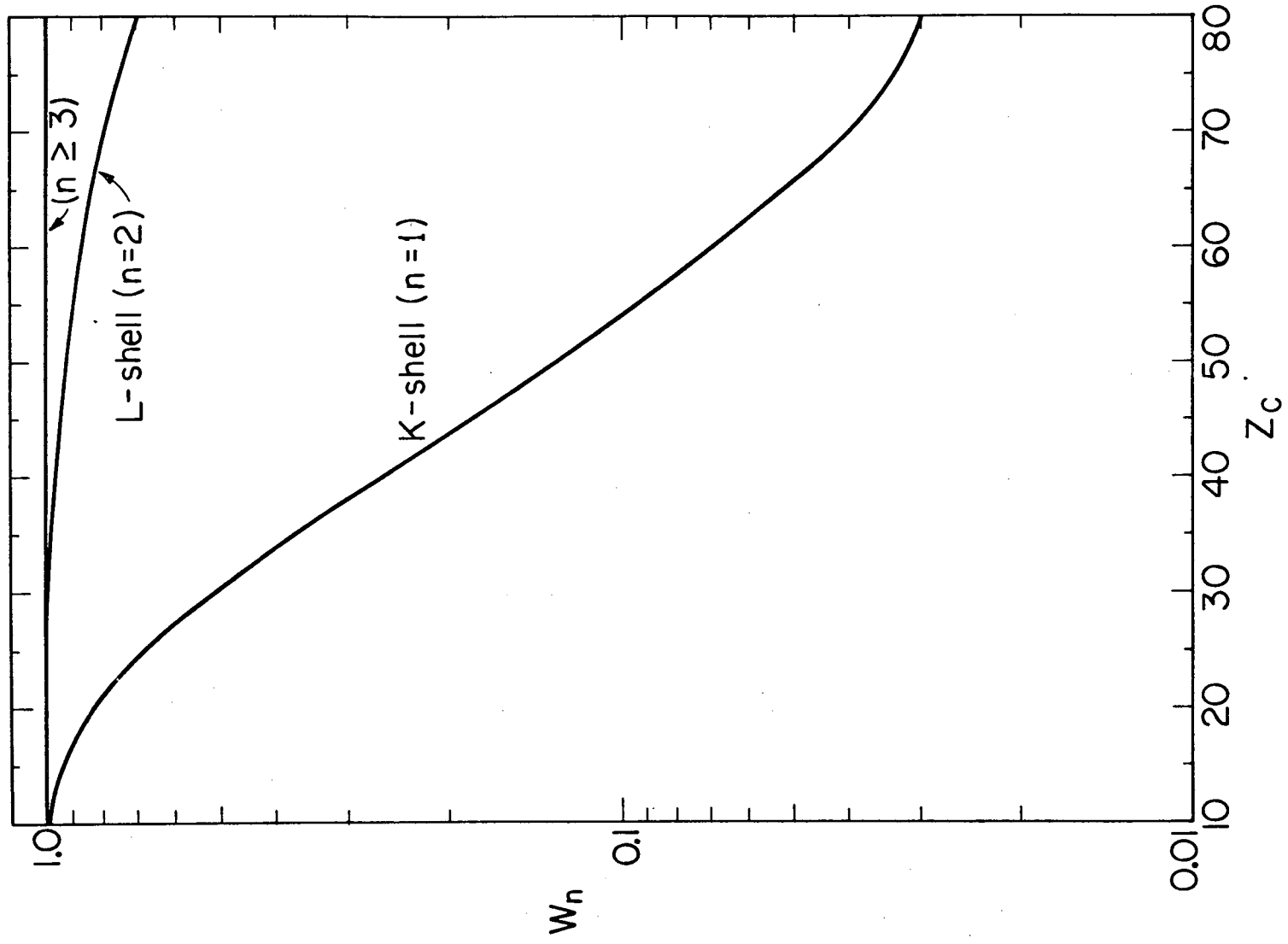
FIGURE CAPTIONS

- Fig. 1. The transition probabilities  $M_D$  to all the allowed bound states and  $M_C$  to all the continuum, at  $Z_C = 30$ . The numbers next to each curve are  $(nl+)$  or  $(nl-)$ . The solid lines are the  $M_D$  values, while the dotted lines are for  $M_C$ .
- Fig. 2. The relative Auger branching ratio as estimated from the fluorescence yield calculations.
- Fig. 3. The estimated ionization cross sections  $\sigma^C$  and  $\sigma^A$  corresponding to the direct excitations to the continuum and the excitations to bound states followed by the Auger emissions, respectively.  $Z = Z_C - Z_I$ , where  $Z_C$  is the core charge and  $Z_I$  is the degree of ionization of the target before the collision. All values are given in  $\pi a_0^2$  units and the electron energy is 20 Mev. The solid lines are the values for  $\sigma^A$ , while the dotted lines are for  $\sigma^C$ .
- Fig. 4. The total ionization cross sections for 20 Mev electron as functions of  $Z_C$  and  $Z = Z_C - Z_I$ . All values are given in  $\pi a_0^2$  units.



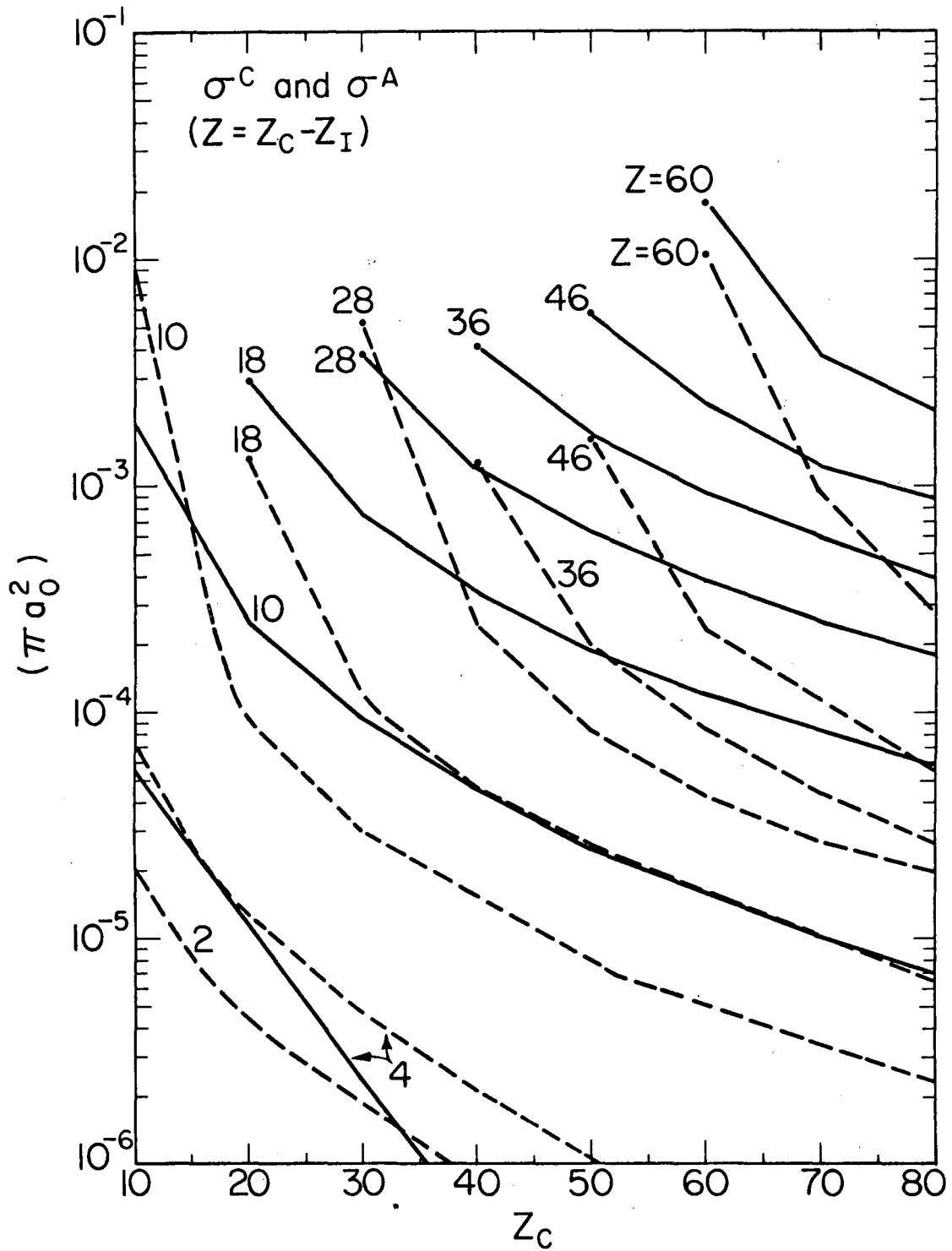
XBL727-3396

Fig. 1



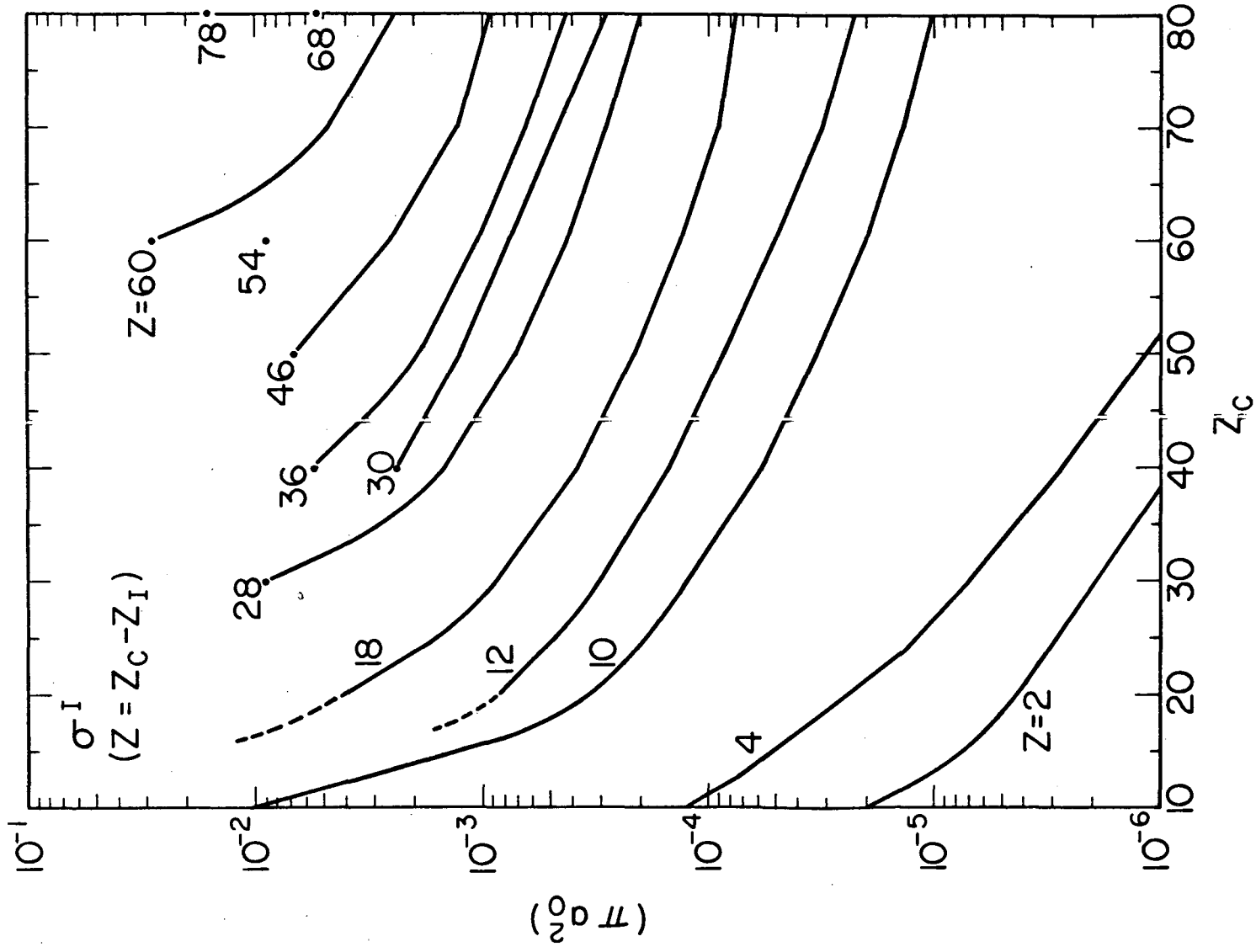
XBL727-3395

Fig. 2



XBL727-3394

Fig. 3



XBL727-3393

Fig. 4



LEGAL NOTICE

*This report was prepared as an account of work sponsored by the United States Government. Neither the United States nor the United States Atomic Energy Commission, nor any of their employees, nor any of their contractors, subcontractors, or their employees, makes any warranty, express or implied, or assumes any legal liability or responsibility for the accuracy, completeness or usefulness of any information, apparatus, product or process disclosed, or represents that its use would not infringe privately owned rights.*

TECHNICAL INFORMATION DIVISION  
LAWRENCE BERKELEY LABORATORY  
UNIVERSITY OF CALIFORNIA  
BERKELEY, CALIFORNIA 94720